

## COMMUNICATION

## A rapid electrochemical method to recycle carbon fiber composites using methyl radicals

Received 00th January 20xx,  
Accepted 00th January 20xx

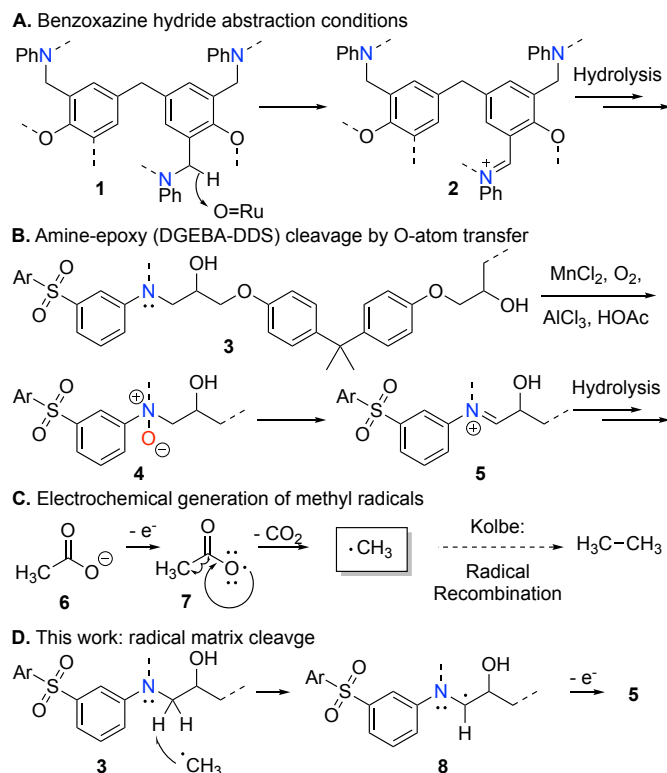
DOI: 10.1039/x0xx00000x

We introduce an electrochemical approach to recycle carbon fiber (CF) fabrics from amine-epoxy carbon fiber-reinforced polymers (CFRPs). Our novel method utilizes a Kolbe-like mechanism to generate methyl radicals from  $\text{CH}_3\text{COOH}$  to cleave C-N bonds within epoxy matrices via hydrogen atom abstraction. Recovered CFs are then remanufactured into CFRPs without resizing.

Thermoset carbon fiber reinforced polymer (CFRP) composites comprise a polymer matrix and carbon fibers (CFs) so that the combination imparts exceptional strength-to-weight, stiffness, and corrosion resistance relative to metallic alloys. Because of these properties, CFRPs are top choices for lightweight structural components in the aerospace, automobile, and wind energy industries. There has been a continuous increase in global demand for CFRPs, projected to reach 285,000 tons in 2025.<sup>1</sup> Thermoset CFRPs are cured irreversibly to produce a solid, crosslinked polymer matrix. Once the process completes, the matrix is insoluble and inert. Thus, recycling end-of-life (EOL) CFRPs is challenging.

We have previously introduced oxidative recycling processes for benzoxazine and amine-epoxy CFRPs, respectively based on ruthenium hydride abstraction<sup>2</sup> and peroxide<sup>3</sup> or  $\text{O}_2/\text{Mn}^{II}$  conditions,<sup>4</sup> each enabling both fiber and resin recovery and featuring analysis of chemical mechanism (Scheme 1ab).<sup>5</sup> Building on these insights, we now present the first electrochemical method to deploy electrolysis-generated methyl radicals to depolymerize amine-epoxy CFRPs (Scheme 1). In this process, we use fibers imbedded within the CFRP as the anode to electrolyze  $\text{CH}_3\text{COOH}$  and generate methyl radicals

directly on the CFRP. Such radicals abstract hydrogen atoms adjacent to the polymer's linking nitrogen atom, thus, ultimately enabling selective C-N bond cleavage and completely dissolving CFRP matrices ( $T_g > 160^\circ\text{C}$ ) within 20 hours while preserving the fabric architecture of CFs. Fiber fabrics were then directly remanufactured into second-cycle CFRPs.



**Scheme 1** Approaches to cleave various CFRP matrices.

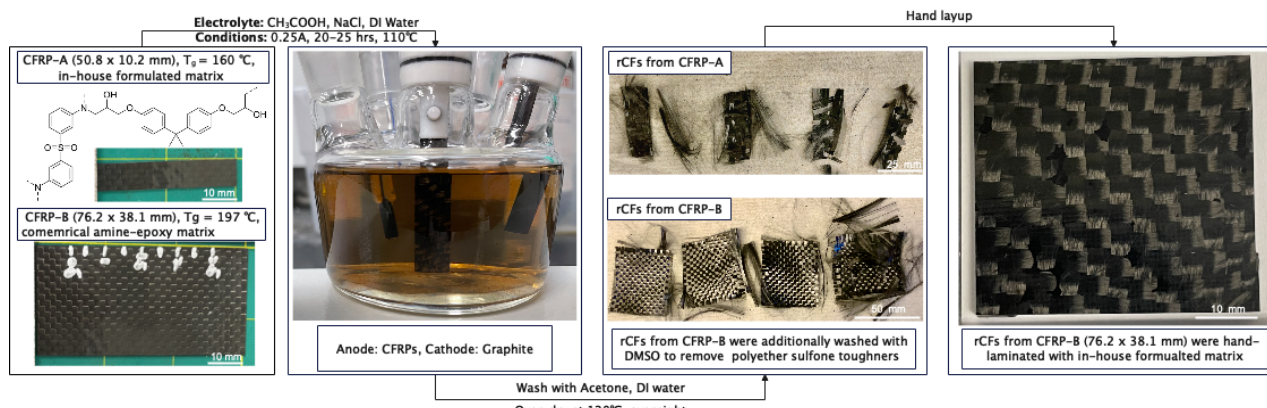
<sup>a,a</sup>MC Gill Composites Center, Mork Family Department of Chemical Engineering and Material Science, University of Southern California, 3651 Watt Way, Los Angeles, California, 90089, USA.

<sup>b,b</sup>Loker Hydrocarbon Research Institute, Wrigley Institute of Environmental Studies, and Department of Chemistry, University of Southern California, 837 Bloom Walk, Los Angeles, California, 90089, USA.

<sup>c</sup>Co-first author.

<sup>d</sup>Co-corresponding author.

<sup>†</sup> Electronic Supplementary Information (ESI) available



**Scheme 2** Electrolysis recycling process for recovering and reusing CFs from amine-epoxy CFRPs

Electrochemical approaches to CFRP recycling have emerged that attempt to leverage the conductive CFs present in the composites. Currently, most electrochemical recycling methods use a CFRP as the anode to electrolyze chloride solutions. These methods reportedly generate chlorine-based oxidants (Cl<sub>2</sub>, HOCl, -OCl) that degrade thermoset polymers and can also chlorinate imbedded fibers.<sup>6-8</sup> Alternative chlorine-free electrochemical methods involve phosphoric acid or a mixture of dimethyl sulfoxide (DMSO) and ammonium acetate.<sup>9, 10</sup> These methods have lower efficiency, taking up to 21 days to complete, and tend to damage the fibers.

Additionally, to our view, no satisfying mechanistic data have been reported on any electrochemical CFRP digest method. Previous studies have shown that photolysis-generated chlorine and hydroxyl radicals digest organic waste.<sup>11</sup> Some CFRP recycling studies have proposed to use radical-based reaction mechanisms to achieve efficient matrix digestion.<sup>12-15</sup> However, these studies did not characterize the reactive intermediate(s) or pathway of depolymerization. Here we will use a spin trap strategy to obtain structural information on our propagating radical(s).

Our method is based on a Kolbe-like electrolysis that generates methyl radicals to cleave C—H groups in an amine-epoxy matrix. Thus, acetic acid decomposes to methyl radicals as shown in Scheme 1c.<sup>16</sup> This happens on the carbon fiber electrode imbedded within the CFRP material. The transient radical mediates a curiously selective hydrogen atom abstraction, ultimately converting the matrix's linking amine to a hydrolysable imine (Scheme 1d).

We demonstrate this concept with two CFRPs, A and B, prepared with different amine-epoxy matrices (see ESI for details). CFRP-A ( $T_g = 160^\circ\text{C}$ ) was produced in-house using di-glycidyl ether of bisphenol A (DGEBA) epoxy and 3,3'-diaminodiphenyl sulfone (3,3'-DDS), as in Scheme 1b. CFRP-B samples ( $T_g = 197^\circ\text{C}$ ) were produced using a commercial prepreg of a similar structure (Solvay CYCOM 5320-1) to demonstrate the feasibility of recovering materials from an aerospace material.

Once fully cured, CFRPs laminates were cut to 50.8 x 10.2 or 76.2 x 38.1 mm for use as the anode, while a graphite rod served as the cathode (Scheme 2). The electrodes were immersed in an electrolyte solution containing CH<sub>3</sub>COOH, NaCl, and deionized

water. Added NaCl assists electron transportation and enhance the conductivity of electrolyte solutions. Electrolysis reactions were performed at constant current (0.25 A) at 110 °C for 20 hours under reflux with various electrolyte concentrations, respectively summarized in Table 1. Entries 1-7 test the effect of NaCl and CH<sub>3</sub>COOH. Entry 8 and 9 demonstrate feasibility of the method on our commercial CFRPs.

**Table 1** Electrolysis CFRP digestion experiment summary

Entry	CFRP	CH <sub>3</sub> COOH(M)	NaCl(M)
1	CFRP-A (50.8 x 10.2 mm)	1.93	1
2	CFRP-A (50.8 x 10.2 mm)	4.35	1
3	CFRP-A (50.8 x 10.2 mm)	6.77	1
4	CFRP-A (50.8 x 10.2 mm)	8.70	1
5	CFRP-A (50.8 x 10.2 mm)	11.6	1
6	CFRP-A (50.8 x 10.2 mm)	11.6	0.75
7	CFRP-A (50.8 x 10.2 mm)	11.6	0.5
8	CFRP-B (50.8 x 10.2 mm)	11.6	1
9	CFRP-B (76.2 x 38.1 mm)	11.6	1

Clean CF fabrics are recovered after electrolysis. Figure 1 shows light microscope images of fabrics recovered after 20 hours using conditions in Table 1. Images of entries 1-5 show more complete matrix removal with increasing CH<sub>3</sub>COOH concentration (1.93-11.6 M) at constant NaCl concentration (1 M). Images of entries 5-8 reveal that increasing NaCl concentration (0.5-1M) resulted in more complete matrix decomposition at constant CH<sub>3</sub>COOH concentration (11.6 M). These show that higher [CH<sub>3</sub>COOH] and [NaCl] reduced digestion times. Therefore, we chose 11.6 M CH<sub>3</sub>COOH and 1 M NaCl (entries 5, 7 and 8).

Figure S2 shows the measured voltage of Table 1, entry 5 fluctuated between 4-6.5 V during the electrolysis. Thus, 4 V was selected as optimal, and we switched conditions to fixed voltage.

Single fiber tensile strengths of fresh and recovered CFs were measured and summarized in Table S2 (see ESI for details). The results show reclaimed CFs retained 94.24% of tensile strength and 83.43% of modulus.

Figure 2 shows SEM images of virgin CF and recovered CFs from entries 5 and 8. Figure 2(a) shows surface grooves

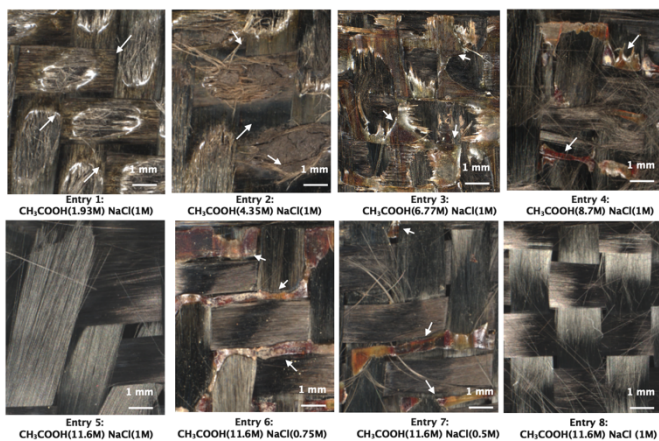


Figure 1 Optical microscope images of recycled CFs from entries 1-8, remaining resin residues (white arrows)

characteristic of the virgin fibers. Figures 2b,c demonstrate that the CFs were clean and undamaged by the electrolysis process. EDS composition analysis of virgin and CFs recovered from entry 5 is summarized in Table 2 and Figure S5-6: after 20 hours of electrolysis, EDS data show no chlorine, and oxygen increased by < 0.8 wt%, indicating no evidence of oxidation or chlorination on recovered CFs. An alternative electrolysis recycling method that involved chlorine reported surface chlorine content increased by up to 8 wt%.<sup>6</sup> The difference in surface chemistry implies that the active radical in our system is carbon-centered, not chlorine or oxygen, as implied elsewhere.

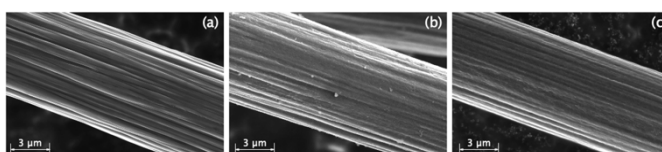


Figure 2 SEM images of virgin CF (a) and recycled CFs from entries 5 (b) and 8 (c)

Table 2 EDS surface element composition analysis summary

Sample	C (wt%)	N (wt%)	O (wt%)
Virgin CF	92.3	6.8	0.9
Recycled CF	93.8	4.5	1.7

Scheme 2 also illustrates the process of recovering CF sheets from CFRP-B and remanufacturing them into second cycle CFRPs. First, CFRP-B (76.2 x 38.1 mm) samples were electrolyzed for 25 hours under optimized conditions. Recovered CF fabrics were washed successively with acetone, deionized water, and DMSO to remove excess reactants and polyether sulfone tougheners. After drying, cleaned fabrics were hand-laminated with in-house resin (as in CFRP-A). Remanufactured CFRPs were fully consolidated, demonstrating the viability of up-cycling intact CF fabric from electrolysis conditions.

We next attempted to spin trap our active radical. This utilizes a nitroxide spin trap to react with any present radicals and produce a long-lived adduct that can be analyzed by EPR and MS.<sup>17</sup> 5,5-dimethyl-1-pyrroline-N-oxide (DMPO) was used to capture and identify radicals. Radicals were generated in the

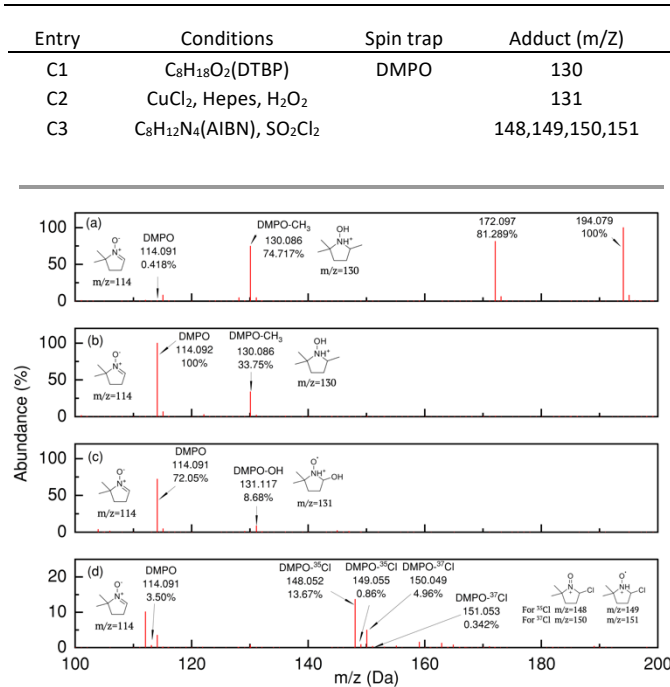
presence and absence of matrix, the latter involving an experiment with a bare CF sheet. Finally, a representative surrogate of the matrix (Bu<sub>4</sub>DDS) was used to confirm that C-N bonds were the cleavage sites.

We first confirmed radical generation. Table 3 shows two trials with the spin trap DMPO using bare fiber (entry A1 and CFRP-A (entry A2) as the anode. EPR confirmed the presence of new radical adducts (Figure S7). Next, we compared the rates of conversion between entries A1 and A2. A sample of each entry was collected after 1 h electrolysis and analyzed by NMR. Despite paramagnetism of the nitroxide radical, structural details of DMPO ring were detectable. Figure S9 shows comparison of the nitroxide signals in (a) pure DMPO, (b) entry A1, and (c) entry A2. The nitroxide signal at  $\delta$  = 7.5 ppm remains in entry A1 but not A2, indicating that the presence of matrix greatly reduces the rate of conversion of DMPO. Thus, the radical is constrained around the matrix. This is supported by COSY NMR data, which also show no nitroxide signal for entry A2 (Figure S10).

Table 3 Active radical trapping experiment summary

Entry	Electrolysis conditions	Spin trap	Anode	Sampling time
A1	CH <sub>3</sub> COOH (11.6M), NaCl (1M), 4V, 60°C	DMPO	CFs	
A2	NaCl (1M), 4V, 60°C	DMPO	CFRP-A	1hr

To identify the propagating radical itself, a sample of entry A1 was analyzed by MS and showed three strong signals at *m/z* = 130, 172, and 194, as illustrated in Figure 3. Positive control experiments were established for the methyl, hydroxyl, and chlorine DMPO radical adducts.

**Table 4** LC-QTOF assignment and positive control experiment**Figure 3** LC-QTOF spectrum of entry A1 (a), C1 (b), C2 (c), and C3 (d). Only entries A1 and C1 display a strong signal for m/z = 130, which confirms the production of methyl radicals.

Using conditions shown in Table 4. Entry C1-3 respectively produced methyl, hydroxyl, and chlorine radicals that were respectively trapped cleanly by DMPO. Figure 3 further shows the stacked mass data for each trapped radical species, including CFRP experiment A1. The signal m/z=130 from A1 aligns only with the methyl radical adduct C1. The finding of methyl radicals is further supported by GC headspace analysis of experiment A1. This exhibits both methane and carbon dioxide (Figure S15), which is consistent with the formation of a methyl radical through a Kolbe-like process (Scheme 1C).

We further identified the site of matrix cleavage by using Bu<sub>4</sub>DDS, a small molecule model of the matrix (Figure S16). Thus, Bu<sub>4</sub>DDS was exposed to our electrolysis system for two hours, using a bare carbon fiber fabric anode. NMR tracked molecular changes; these conditions are laid out in Table 5 and Figure S17. We note a decrease in a signal at  $\delta$  = 3.29, which is characteristic of the R<sub>2</sub>N-CH<sub>2</sub>R group. The corresponding appearance of a  $\delta$  = 2.98 signal represents mono-dealkylated Bu<sub>3</sub>DDS and N,N'-Bu<sub>2</sub>DDS. We surmise that these form via C—H atom abstraction, followed by oxidation to an iminium cation that hydrolyzes readily. Interestingly, while dealkylation proceeds all the way to primary anilines, no further degradation is observed. This was proven when we attempted to digest DDS and isolated unreacted DDS and acetylated DDS derivatives, the latter acetylated by the solvent (Figure S18 and S19).

**Table 5** Bu<sub>4</sub>DDS small molecule matrix model digestion experiment summary

Entry	Electrolysis conditions	Matrix	Anode	Sampling time
B1	CH <sub>3</sub> COOH (11.6M),			1hr
B2	NaCl (1M) 4V,60°C	Bu <sub>4</sub> DDS	Graphite	2hr

Our combined data lead to a proposed mechanism for this process, shown in Scheme 1D. Methyl radicals are the active oxidant in the system, cleaving the R<sub>2</sub>N-CH<sub>2</sub>R bond by an initial hydrogen atom abstraction. This leads to iminium hydrolysis and selective bond cleavage at the polymeric C—N linkage.

In summary, we report an efficient electrochemical CFRP recycling method. Careful mechanistic studies hold that the process exploits methyl radicals, derived from solvent electrooxidation, selectively to depolymerize amine-epoxy matrices to form recoverable fine chemicals. Unlike prior electrochemical methods, this radical-based technology achieves complete dissolution of high-performance CFRPs within 20 hours and yields clean CFs that are readily remanufactured into second-generation CFRPs. We confirm the presence of methyl radicals with the first application of spin trapping methodology in CFRP recycling. The study provides a new chemical recycling pathway using radicals to up-cycle high-performance composites.

## Conflicts of interest

T. J. Williams is the founder of Closed Composites, a start-up aiming to commercialize composite materials recycling.

## Acknowledgement

This work is sponsored by the MC Gill Composites Center at USC and the National Science Foundation (CMMI-2134658). and TJW thanks NSF for BRITE award sponsorship (CMMI-2227649). We thank the NSF (CHE-2018740, DBI-0821671, CHE-0840366), the NIH (S10 RR25432), and USC Research and Innovation Instrumentation Awards for analytical tools. Huntsman Corporation and Solvay generously donated the epoxy, amine curing agent, and prepreg used in this study. We thank Brian Feng for taking SEM and EDS characterization and Jaideep Singh for EPR characterization.

## Notes and references

1. J. Zhang, G. Lin, U. Vaidya and H. Wang, *Composites Part B: Engineering*, 2022, 110463.
2. J. N. Lo, S. R. Nutt and T. J. Williams, *ACS Sustainable Chemistry & Engineering*, 2018, **6**, 7227-7231.
3. Y. Ma, D. Kim and S. R. Nutt, *Polymer Degradation and Stability*, 2017, **146**, 240-249.
4. C. A. Navarro, Y. Ma, K. H. Michael, H. M. Breunig, S. R. Nutt and T. J. Williams, *Green Chemistry*, 2021, **23**, 6356-6360.
5. C. A. Navarro, E. A. Kedzie, Y. Ma, K. H. Michael, S. R. Nutt and T. J. Williams, *Topics in Catalysis*, 2018, **61**, 704-709.
6. H. Sun, G. Guo, S. A. Memon, W. Xu, Q. Zhang, J.-H. Zhu and F. Xing, *Composites Part A: Applied Science and Manufacturing*, 2015, **78**, 10-17.
7. J.-H. Zhu, P.-Y. Chen, M.-N. Su, C. Pei and F. Xing, *Green Chemistry*, 2019, **21**, 1635-1647.
8. K. Oshima, S. Matsuda, M. Hosaka and S. Satokawa, *Separation and Purification Technology*, 2020, **231**, 115885.

9. K. Oshima, M. Hosaka, S. Matsuda and S. Satokawa, *Separation and Purification Technology*, 2020, **251**, 117296.
10. C. Pei, P.-Y. Chen, S.-C. Kong, J. Wu, J.-H. Zhu and F. Xing, *Separation and Purification Technology*, 2021, **278**, 119591.
11. S. Xiao, J. Qu, X. Zhao, H. Liu and D. Wan, *Water Research*, 2009, **43**, 1432-1440.
12. M. Das, R. Chacko and S. Varughese, *ACS Sustainable Chemistry & Engineering*, 2018, **6**, 1564-1571.
13. A. Yu, Y. Hong, E. Song, H. Kim, I. Choi and M. Goh, *Journal of Industrial and Engineering Chemistry*, 2022, **112**, 193-200.
14. D. H. Kim, M. Lee and M. Goh, *ACS Sustainable Chemistry & Engineering*, 2020, **8**, 2433-2440.
15. M. Lee, D. H. Kim, J.-J. Park, N.-H. You and M. Goh, *Waste Management*, 2020, **118**, 190-196.
16. F. J. Holzhäuser, J. B. Mensah and R. Palkovits, *Green Chemistry*, 2020, **22**, 286-301.
17. M. J. Davies, *Methods*, 2016, **109**, 21-30.

## Supplementary Materials

### A rapid electrochemical method to recycle carbon fiber composites using methyl radicals

Zehan Yu,<sup>a,c</sup> Justin Lim,<sup>b,c</sup> Travis J. Williams,<sup>b,\*</sup> and Steven R. Nutt<sup>a,\*</sup>

<sup>a</sup>*Department of Chemical Engineering and Materials Science, University of Southern California*

<sup>b</sup>*Loker Hydrocarbon Research Institute, Wrigley Institute for Environment and Sustainability,  
and Department of Chemistry, University of Southern California*

<sup>c</sup>*Co-first Author*

*\*Co-Corresponding Author: [travisw@usc.edu](mailto:travisw@usc.edu)*

*\*Co-Corresponding Author: [nutt@usc.edu](mailto:nutt@usc.edu)*

- 1. General Procedures**
- 2. Electrolysis CFRP digestion experiment procedure**
  - a. Preparation of fully cured amine-epoxy CFRPs
  - b. Electrolysis digestion experiments
  - c. Remanufacture CFRP using recovered CFs
- 3. Single fiber tensile test of virgin and electrolysis recycled CFs**
- 4. EDS spectrum of virgin and electrolysis recycled CFs**
- 5. EPR spectrum of captured radicals in the electrolyzed system**
- 6. Supporting NMR spectrum for active radical detection experiments:**
  - a.  $^1\text{H}$  NMR spectrum of 5,5-dimethyl-1-pyrroline-*N*-oxide (DMPO)
  - b.  $^1\text{H}$  NMR stacked spectra of A1 and A2
  - c. COSY spectra of A1 and A2 – conversion of nitrone signal
- 7. MS from DMPO spin trap experiments**
  - a. Entry A1 radical detection experiment
  - b. DMPO-Hydroxyl adduct positive control
  - c. DMPO-Chlorine adduct positive control
  - d. DMPO-Methyl adduct positive control
- 8. GC analysis of electrolysis headspace**
- 9. Supporting NMR spectrum for active radical detection experiments:**
  - a.  $^1\text{H}$  NMR of compound Bu<sub>4</sub>DDS
  - b.  $^1\text{H}$  NMR stacked spectra of Bu<sub>4</sub>DDS digestion in electrolyzed system
  - c.  $^1\text{H}$  NMR stacked spectra of DDS digestion in electrolyzed system
  - d. MS spectrum of DDS digestion in electrolyzed system for 1 hour

## 1. General Procedures

All synthetic procedures were conducted in a chemical fume hood with exposure to air, unless otherwise indicated. Deuterated NMR solvents were purchased from Cambridge Isotopes Laboratories. 5,5-Dimethyl-1-pyrroline-*N*-oxide (DMPO) was supplied by Supelco. Unless otherwise specified, chloroform and all reagents (including sulfonyl chloride and AIBN) are commonly available from major commercial suppliers (Sigma-Aldrich, Merck, Fischer Scientific, TCI America, Acros Organics) and used without further purification. Dichloromethane, acetonitrile and hexanes are purchased from VWR and dried in a J. C. Meyer solvent purification system with alumina/copper (II) oxide columns; dichloromethane was dried by vacuum transfer from a calcium hydride suspension. Deionized water was purified in-house using a deionizer cartridge (Philadelphia Scientific).

NMR spectra were recorded on a Varian Mercury 400, Varian VNMRS 500, or VNMRS 600, spectrometers processed using MestReNova. All chemical shifts are reported in units of ppm and referenced to the residual  $^1\text{H}$  or  $^{13}\text{C}$  solvent peak and line-listed according to (s) singlet, (bs) broad singlet, (d) doublet, (t) triplet, (dd) double doublet, etc.  $^{13}\text{C}$  spectra are delimited by carbon peaks, not carbon count. Air-sensitive NMR spectra were taken in 8" J-Young tubes (Wilmad or Norell) with Teflon valve plugs. Mass spectral data were acquired on an Agilent 6545 LC-QTOF instrument with electrospray set to positive ionization.

Pre-impregnated resin-fiber substrate materials, "prepregs" were fabricated in house or sourced from Solvay according to specified procedures. Cured CRFP panels were cut with a water jet cutter (ProtoMAX) as described.

Electrolysis was mediated with a Hanmatek HM310P potentiostat using the reactor described below and pictured in Figure 1 of the main text.

Images were recorded using a digital stereo microscope (Keyence VHX-5000). SEM images were taken on a Helios G4 FIB/SEM (Thermo Scientific). EDS spectra were recorded on the Helios G4 FIB/SEM using Oxford UltimMax 170 Silicon Drift detector.

## 2. Electrolysis digestion experiment procedures:

### a. Preparation of fully cured amine-epoxy CFRPs:

Epoxy equivalent weight (EEW) and amine hydrogen equivalent weight (AHEW) were used to calculate the mixing ratio of amine/epoxy. A resin of CFRP-A was formulated using the bifunctional epoxy diglycidyl ether of bisphenol A (17.95 g, EEW = 187 g/eq, Araldite GY 6010, Huntsman) and tetra-functional amine curing agent (6.05 g, 3,3'-diaminodiphenyl sulfone, AHEW = 63 g/eq, Aradur 9719-1, Huntsman). The mixing ratio of amine/epoxy was 100% (molar). After hand mixing epoxy and amine for 10 mins, the mixture was transferred into a vacuum oven (set at 120 °C) to vacuum degassing. After 10 mins, the mixture became clear and homogenous. A resin film was then prepared by spreading liquid resin onto a 203 x 203 mm release film (Airtech, Release Ease 236 TFNP), preheating at 50 °C on Wabash hot press. Prepreg was fabricated using 2 X 2 twill weave CF fabrics (FiberGlast 1069-B). One resin film was attached to each side of the CF fabric. Then, the stack was heated and pressed using a hot press at 50 °C with 20 kPa pressure for 1 min. CFRP-A panels were then laminated via a vacuum bag-only process (VBO) using 4 plies of prepreg. The curing cycle was (1) 1.5 °C/min to 120 °C, (2) hold at 120 °C for 3 hrs, (3) 1.5 °C/min to 180 °C and (4) hold at 180 °C for 3 hrs. Fully cured CFRP-A panels were then cut to 50.8 x 10.2 mm using a water-jet cutter.

CFRP-B panels were fabricated using 4 plies of aerospace-grade VBO prepreg (Solvay CYCOM 5320-1, T650, PW). The cure cycle was (1) hold at 60 °C for 2 hrs, (2) 1 °C/min to 120 °C, (2) hold at 120 °C for 2 hrs, (3) 1.7 °C/min to 177 °C, and (4) hold at 177 at 120 °C for 2 hrs. Fully cured CFRP-B panels were cut into 50.8 x 10.2 mm or 76.2 x 38.1 mm samples on a water-jet cutter.

### b. Electrolysis digestion experiments

A CFRP sample was clamped by a PTFE (Teflon) platinum electrode holder and connected to a DC potentiostat as an anode, while a graphite rod served as the cathode as pictured in the main text and diagrammed in Figure S1. The electrodes were immersed in the electrolyte solution containing CH<sub>3</sub>COOH, NaCl, and DI water, according to loading details that are listed in Table 1 of the main text. For a 50.8 x 10.2 mm CFRP samples, 38.1 mm of the sample was immersed in solution and electrolyzed. Electrolysis reactions were performed in 180 mL electrolyte, using a 200 mL 5-neck glass vessel at reflux. For 76.2 x 38.1 mm CFRP samples, 44.4 mm of the sample was immersed in solution and electrolyzed. Electrolysis reactions were conducted in 250 mL electrolyte, using a 250 ml 4-neck glass vessel with a removal lid at reflux.

After electrolysis, reacted CF weaves of CFRP samples were cut using scissors. Then, the CF weaves were cleaned using water and acetone to remove excess reactants. CFRP-B samples were additionally washed by dimethyl sulfoxide (DMSO) to remove polyether sulfone hardener. Cleaned CFs fabrics were then dried at 130°C overnight in a convection oven.

Table S1: Electrolysis CFRP digestion experiment electrolyte summary

Entry	CH <sub>3</sub> COOH (ml, mol)	CH <sub>3</sub> COOH (M)	NaCl (g, mol)	NaCl (M)	DI water(ml)
1	20, 0.35	1.93	10.52, 0.18	1	160
2	45, 0.78	4.35	10.52, 0.18	1	135
3	70, 1.22	6.77	10.52, 0.18	1	110
4	90, 1.57	8.70	10.52, 0.18	1	90
5	120, 2.09	11.6	10.52, 0.18	1	60
6	120, 2.09	11.6	7.89, 0.14	0.75	60
7	120, 2.09	11.6	5.26, 0.09	0.5	60
8	120, 2.09	11.6	10.52, 0.18	1	60
9	167, 2.91	11.6	14.61, 0.25	1	83

### c. Remanufactured CFRPs using recovered CFs

Recovered CF weaves (44.4 x 38.1 mm) and in-house formulated resin were used to remanufacture CFRPs. Loose fibers were removed or organized from the recovered weaves. Then, a layer of resin was applied to the recovered CF fabric using a brush, and a new ply of CF weaves is placed on top. The process was repeated for all 4 plies in the laminate. Then, the stack was cured via a VBO process using the same curing cycle as the CFRP-A sample.

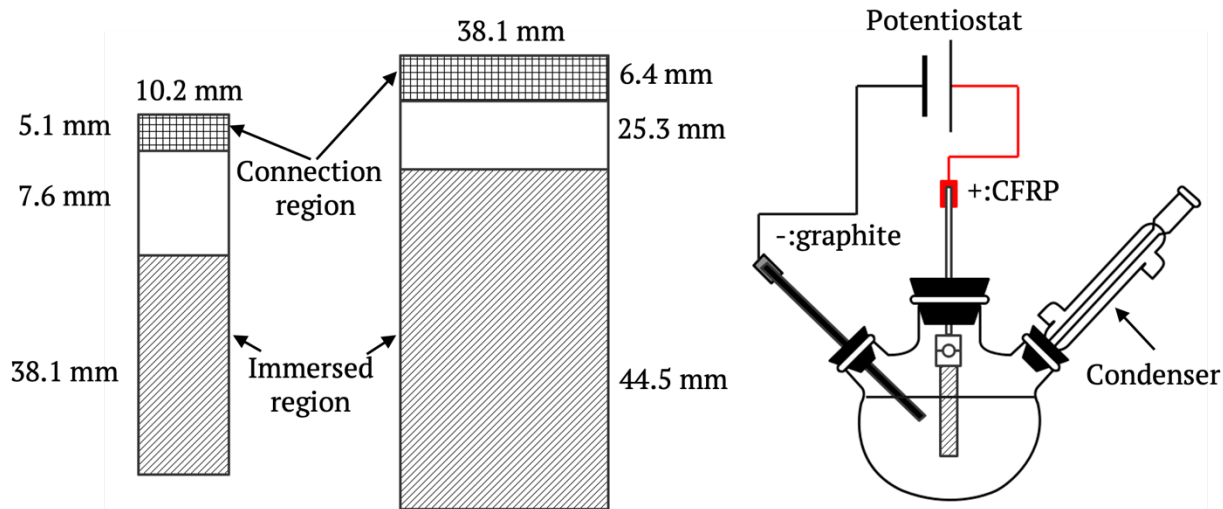


Figure S1: (a) CFRP samples 50.8 x 10.2 mm, (b) 76.2 x 38.1 mm, and (c) schematic of electrolysis recycling setup

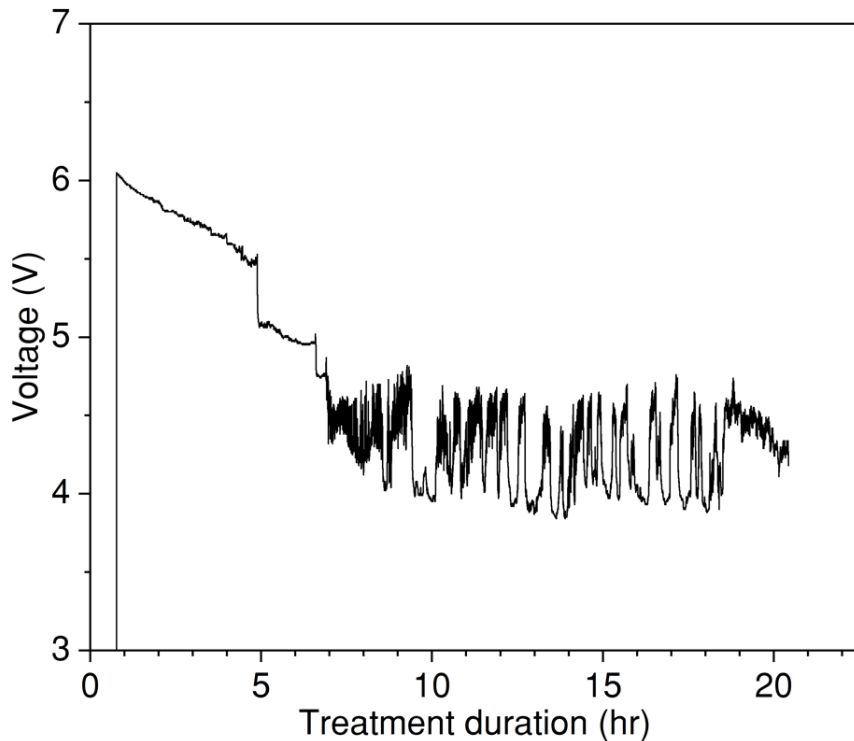


Figure S2: Measured voltage of Table 1, entry 5 (main text) during the electrolysis digestion

### 3. Single fiber tensile tests of virgin and electrolysis recycled CFs

CFRs were laminated using 2 x 2 twill weave CF fabrics (FiberGlast 1069-B), and Solvay CYCOM 5320-1 resin films. Fully cured panels were cut into 79.25 x 10.16 mm samples. CFRP samples were electrolyzed in 200ml electrolyte (11.6M CH<sub>3</sub>COOH, 1M NaCl) at 110°C for 20hrs. Recovered CFs were cleaned using DI water, acetone, and DMSO. Cleaned CFs were dried in a convection oven at 120°C overnight before testing.

The tensile properties of electrolysis-recycled CFs, and virgin fibers were tested and summarized in Table S2. A total of 44 tests were conducted, with 22 tests performed separately on the virgin and recycled CFs, following the IOS 11566 standard. The tensile strength for the fresh and electrolysis-recycled CFs were 2976.02 MPa and 2804.72 MPa. The modulus for the fresh and electrolysis-recycled CFs were 178.59 GPa and 149.01 GPa. Electrolysis-recycled CFs retained 94.24% of tensile strength and 83.43% of modulus.

Table S2: Single fiber tensile test summary of fresh and electrolysis-recycled CFs

Samples	Break Force(N)	STDEV	Strength (MPa)	STDEV	Modulus (GPa)	STDEV
Fresh CFs	0.1340	0.0265	2976.02	592.62	178.59	18.84
Electrolysis-recycled CFs	0.1266	0.0282	2804.72	644.30	149.01	19.68
Retention (%)	94.48		94.24		83.43	

Sample mounting sheets were cut from printer paper into 25.4 x 76.2 mm strips with a 15.24 x 20.32 mm window in the center. Single fibers were separated from tows and mounted across the window of the mounting papers. Both sides of single fibers were affixed using double-sided tapes and epoxy adhesive (Henkel E-120HP) to secure the fibers in place.

Once the epoxy adhesive had cured, the mounted samples were examined using a light microscope (Keyence VHX-5000) using a 1000X lens to measure fiber diameter. The diameter of each sample was measured three times, and the resulting measured values were averaged to obtain the final measurement.

After mounting the sample onto the load frame, a cut was made in the center of the mounting sheet to free the fiber for testing. The samples were tested at 2mm/min crosshead speed till break. A total of 44 tests were conducted, with 22 tests performed on fresh CFs and another 22 tests on electrolysis-recycled CFs.

The CF cross-sections were assumed to be circular, and the areas were calculated using the diameters previously measured on the light microscope. The tensile strength was then calculated and plotted against strain (%) using these calculated areas. The slope of stress-strain curves was taken as tensile modulus. Table S3-4 summarize all tensile test results.

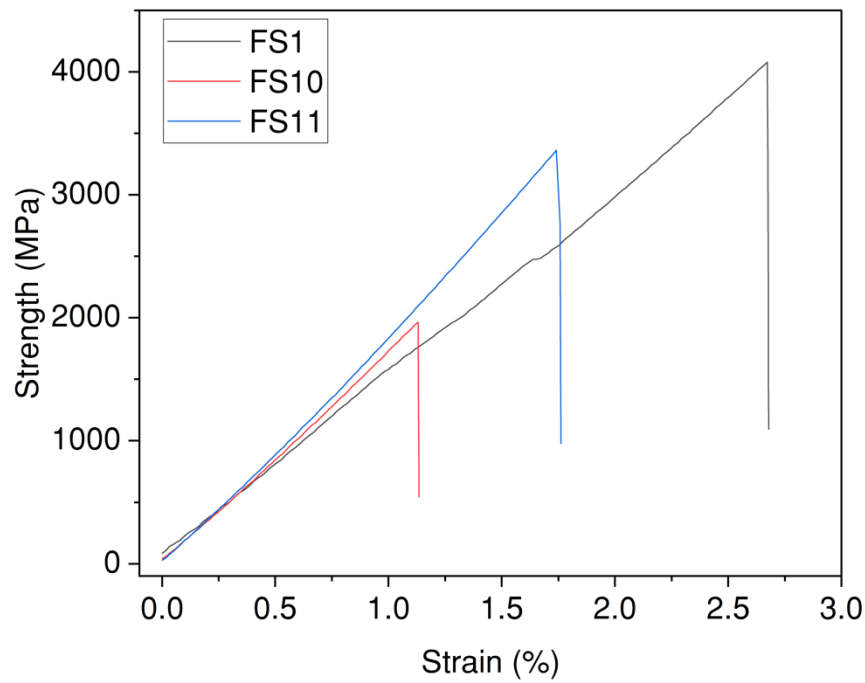


Figure S3: Representative stress-strain curves from tensile tests on fresh CF

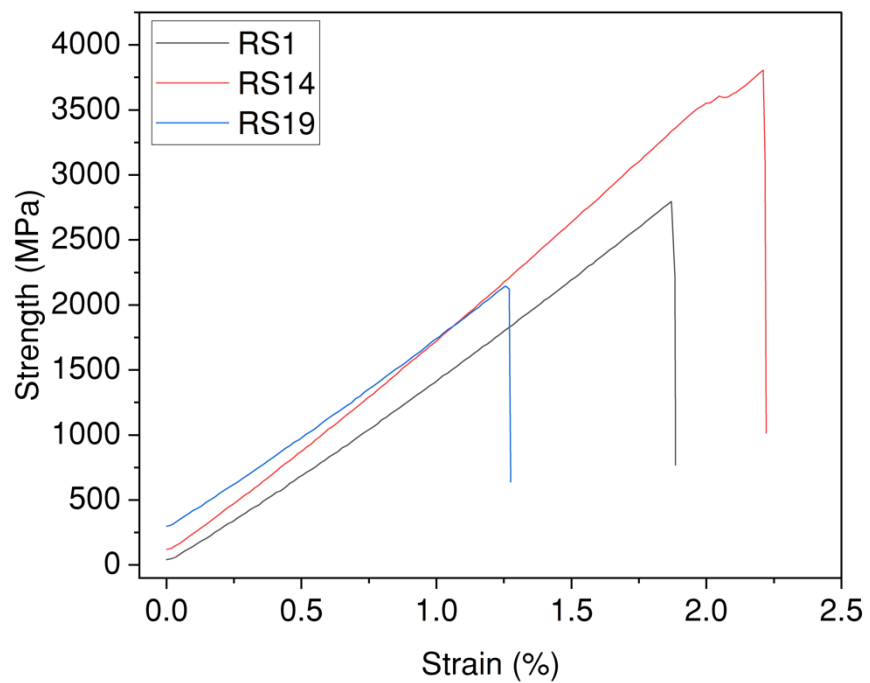


Figure S4: Representative stress-strain curves from tensile tests on electrolysis-recycled CF

*Table S3: Summary of fresh CFs tensile tests*

Sample	Break Force (N)	Diameter ( $\mu\text{m}$ )	Tensile Strength (MPa)	Modulus (GPa)
FS1	0.1785	7.5	4078.87	146.78
FS2	0.1092	7.4	2516.44	159.02
FS3	0.1264	7.6	2811.68	160.84
FS4	0.1757	7.6	3909.47	158.20
FS5	0.1531	7.5	3467.91	165.10
FS6	0.1164	7.5	2612.82	159.39
FS7	0.0886	7.6	1937.90	154.97
FS8	0.1497	7.5	3359.18	172.30
FS9	0.1277	7.6	2815.74	185.45
FS10	0.0876	7.5	1966.35	171.52
FS11	0.1525	7.6	3363.14	192.72
FS12	0.1364	7.6	3007.83	178.85
FS13	0.1460	7.5	3306.44	213.58
FS14	0.0994	7.5	2270.33	184.21
FS15	0.1202	7.6	2673.51	189.06
FS16	0.1628	7.7	3527.48	218.13
FS17	0.1542	7.6	3400.41	191.06
FS18	0.1681	7.6	3675.98	198.58
FS19	0.1245	7.6	2770.51	191.79
FS20	0.1070	7.8	2258.61	185.06
FS21	0.1355	7.7	2911.09	166.94
FS22	0.1295	7.6	2830.77	185.49
AVG	0.1340	7.6	2976.02	178.59
STDEV	0.0265	0.1	592.62	18.84

*Table S4: Summary of electrolysis-recycled CFs tensile tests*

Sample	Break Force (N)	Diameter (μm)	Tensile Strength (MPa)	Modulus (GPa)
RS1	0.1246	7.5	2797.11	149.10
RS2	0.0849	7.8	1776.82	115.45
RS3	0.1073	7.6	2366.48	140.73
RS4	0.1076	7.6	2404.63	113.43
RS5	0.0801	7.4	1846.24	137.32
RS6	0.1081	7.9	2225.43	121.99
RS7	0.0821	7.5	1859.31	116.35
RS8	0.1320	7.6	2911.01	154.32
RS9	0.1428	7.6	3149.43	164.05
RS10	0.1652	7.5	3773.60	171.67
RS11	0.1580	7.6	3485.54	172.44
RS12	0.1310	7.7	2838.93	156.75
RS13	0.1486	7.6	3249.00	162.49
RS14	0.1726	7.6	3806.88	174.37
RS15	0.1557	7.6	3464.25	174.66
RS16	0.1452	7.5	3318.21	155.21
RS17	0.1545	7.5	3468.04	162.21
RS18	0.1392	7.5	3180.42	141.54
RS19	0.0973	7.6	2145.71	148.85
RS20	0.1359	7.6	2996.81	162.90
RS21	0.1218	7.7	2639.76	153.38
RS22	0.0915	7.6	2000.21	128.95
AVG	0.1266	7.6	2804.72	149.01
STDEV	0.0282	0.1	644.30	19.68

#### 4. EDS images of the reclaimed carbon fiber surface

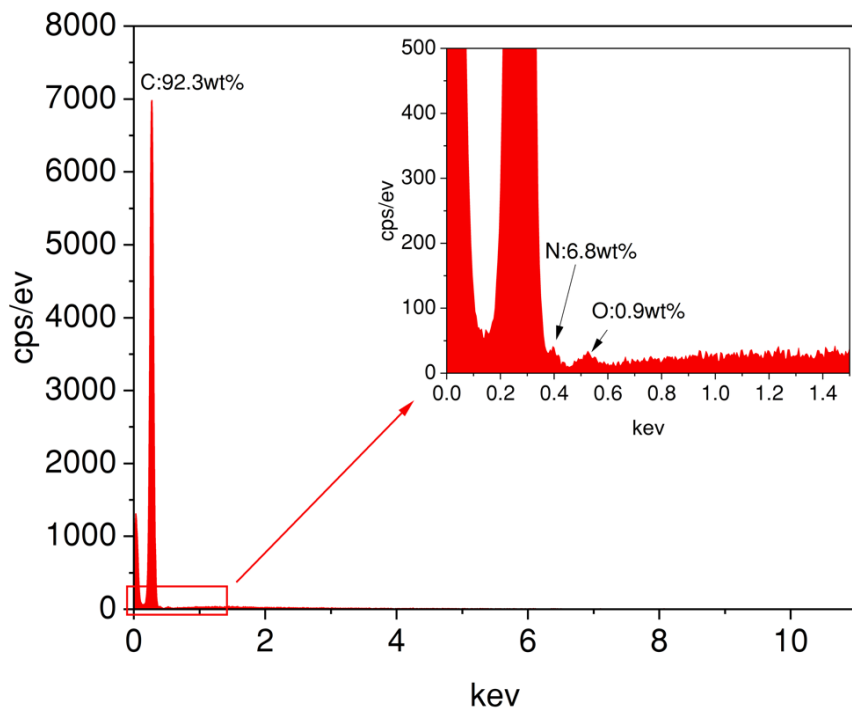


Figure S5: EDS spectrum of virgin CF

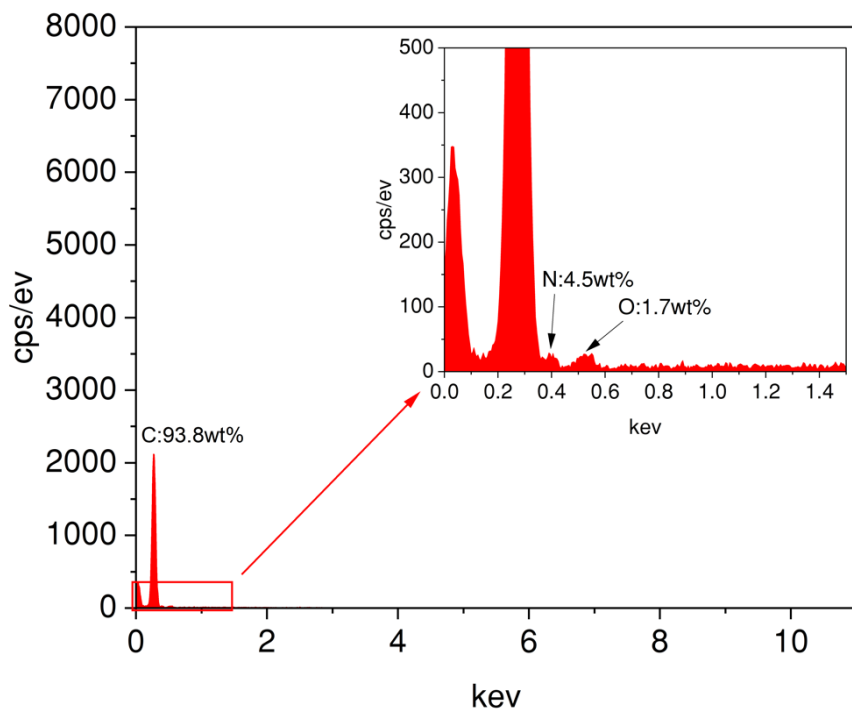


Figure S6: EDS spectrum of recycled CF from main text Table I entry 5

## 5. EPR spectrum of captured radicals in the electrolyzed system

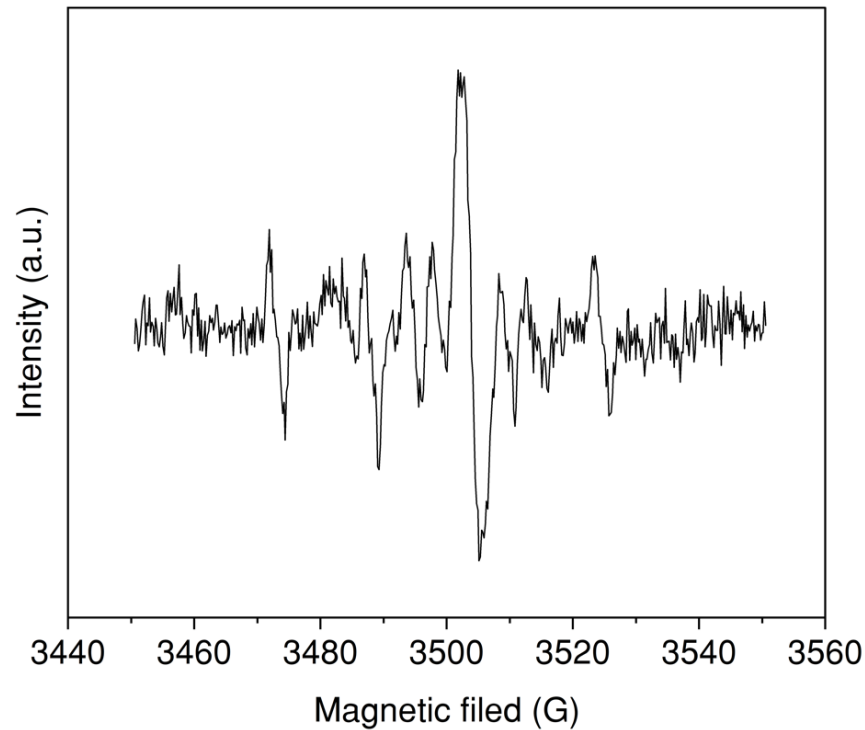


Figure S7: EPR spectrum of the product of Table 3, entry A1 (main text)

6. Supporting NMR spectrum for active radical detection experiments:

a.  $^1\text{H}$  NMR spectrum of 5,5-dimethyl-1-pyrroline-*N*-oxide (DMPO)

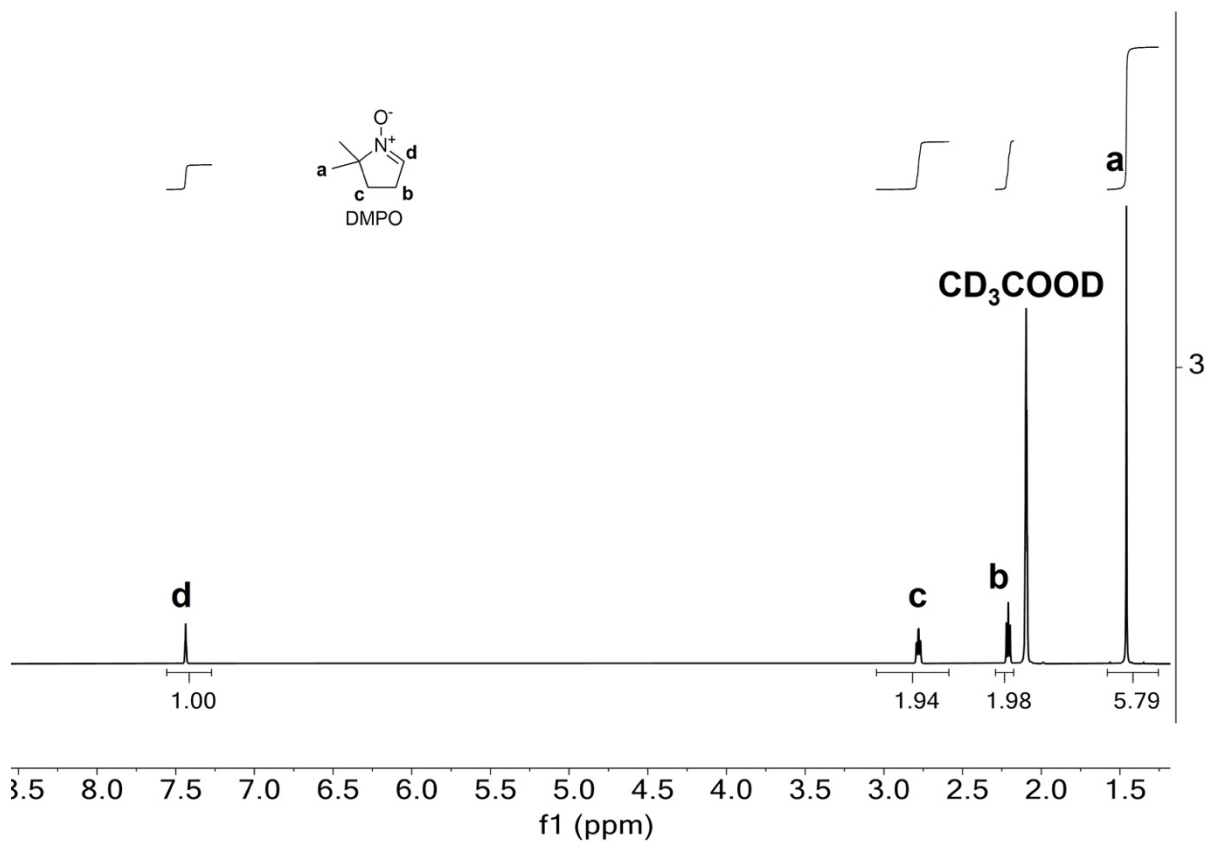


Figure S8:  $^1\text{H}$  NMR spectrum of commercial DMPO

$^1\text{H}$  NMR (600 MHz, acetic acid)  $\delta$  7.44 (t,  $J = 2.5$  Hz, 1H), 2.78 (td,  $J = 7.4, 2.5$  Hz, 2H), 2.21 (t,  $J = 7.4$  Hz, 2H), 1.46 (s, 6H).

**b.  $^1\text{H}$  NMR stacked spectra of DMPO digestion in electrolyzed system**

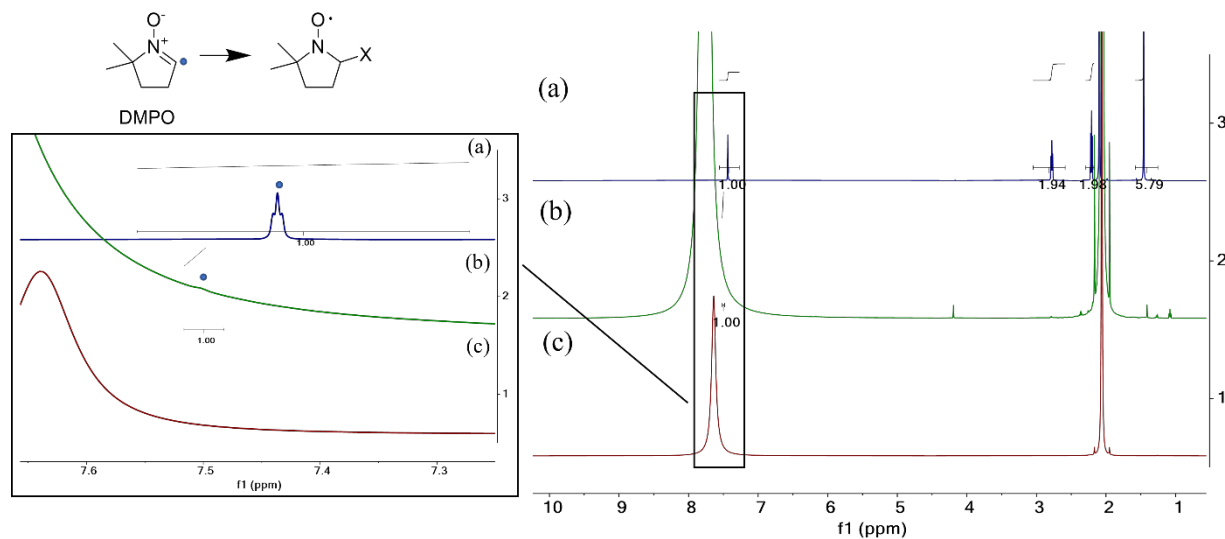


Figure S9: Stacked  $^1\text{H}$  NMR spectrum of main text Table 3, entries A1 and A2

**c. COSY spectra of products of Table 3 (A1 and A2)**

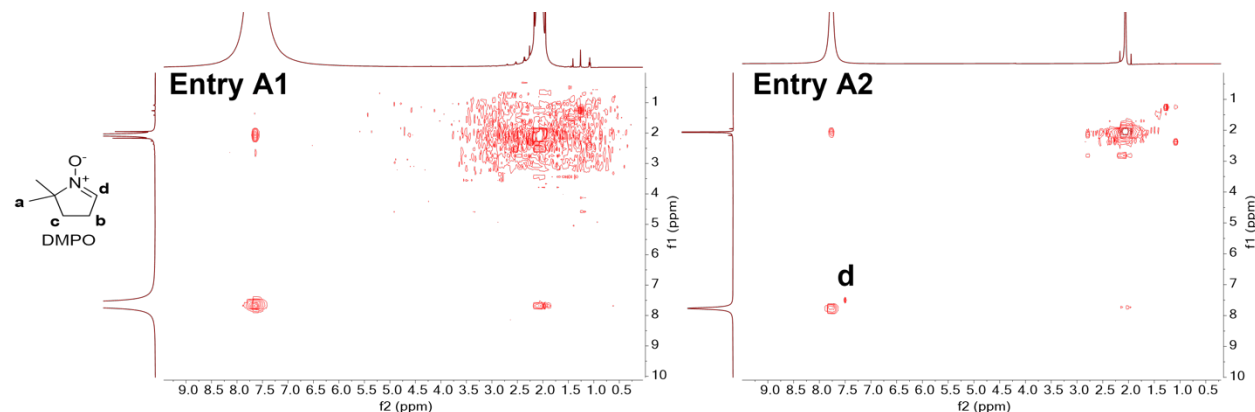
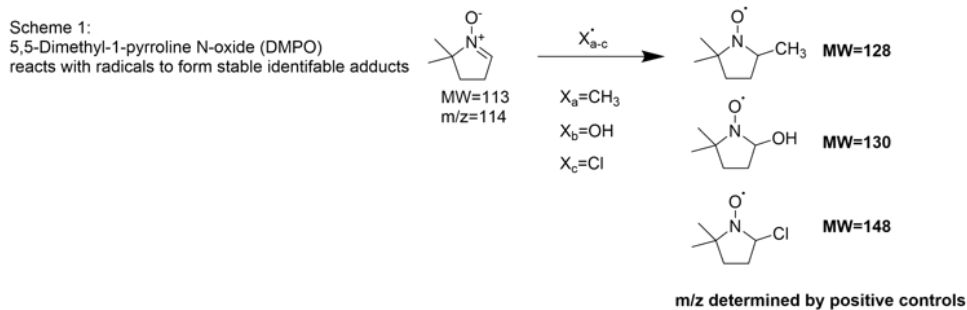


Figure S10: COSY NMR spectrum of main text Table 3, entries A1 and A2

## 7. Mass spectra from DMPO spin trap experiments

### a. Main text Table 3, entry A1

In the 5-neck glass electrolysis vessel (main text scheme 2), acetic acid (10 mL, 17.4 M) and NaCl (876.6 mg, 1 M) were dissolved in deionized water (5 mL). The electrolysis apparatus was assembled as described above, and a voltage of 4 V was applied. The vessel was flushed with argon gas and allowed to react for 5 minutes. The solution was then heated to 65 °C and DMPO (15.0 mg, 31.3  $\mu$ mol, 8.84 mM) was added. A sample aliquot was collected after 60 minutes.



*Scheme S1: Active radical trap experiment and identification protocol*

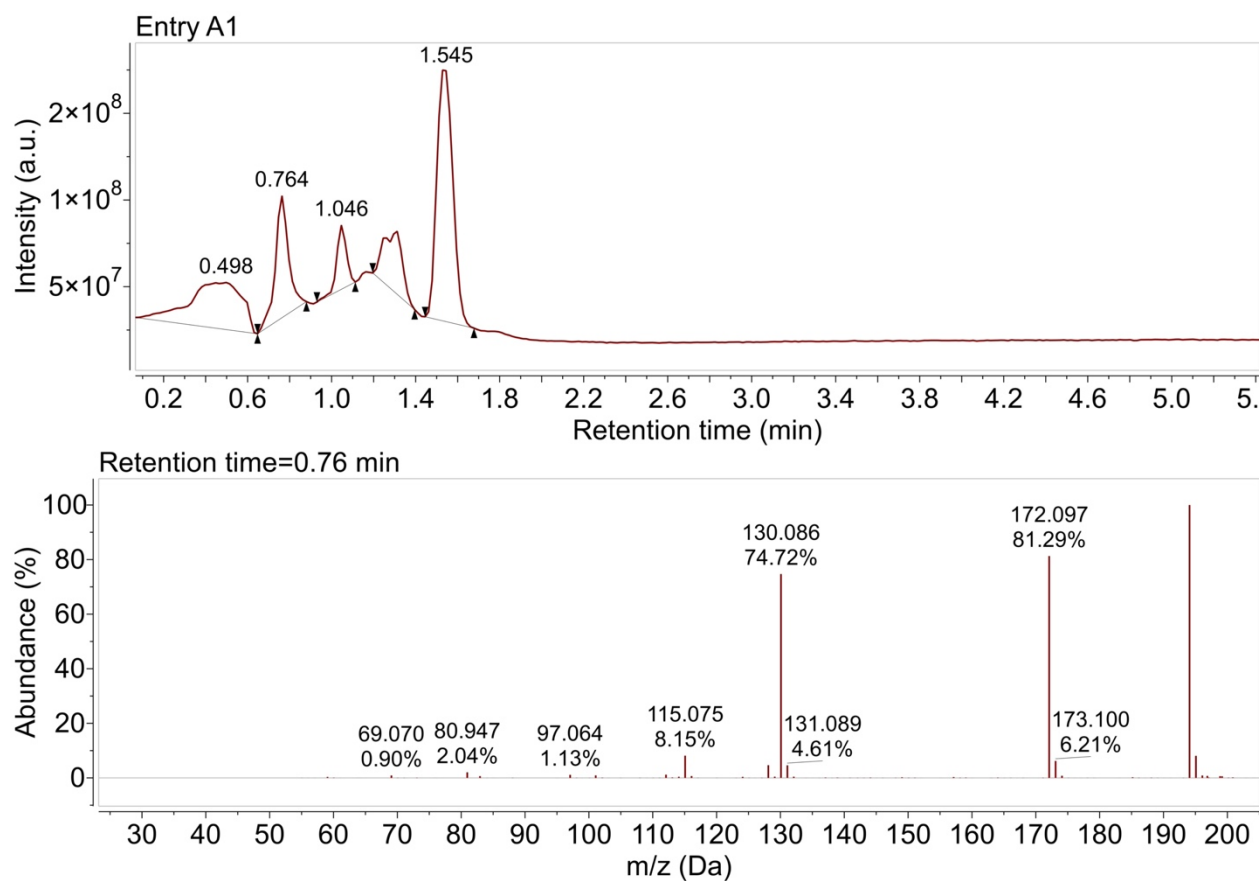
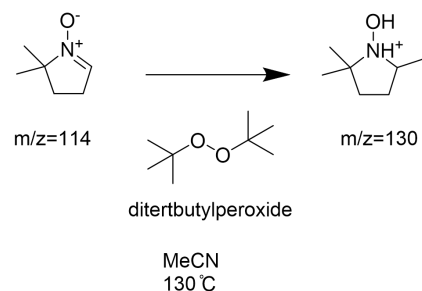


*Figure S11: Mass spectrum of Table 3, entry A1 (main text). MS profile for RT = 0.76 min*

### b. DMPO-Methyl adduct Positive Control

In a 5 mL oven dried round bottom flask were combined acetonitrile (1.0 mL) and ditertbutylperoxide (7.0 mg, 38  $\mu$ mol). The solution was heated to 130 °C, then after two minutes DMPO (10 mg, 8.9  $\mu$ mol) was added into the solution (8.85 mM). The resulting solution was heated for 1 hour before the heat was turned off.



*Scheme S2: DMPO-methyl adduct positive control experiment*

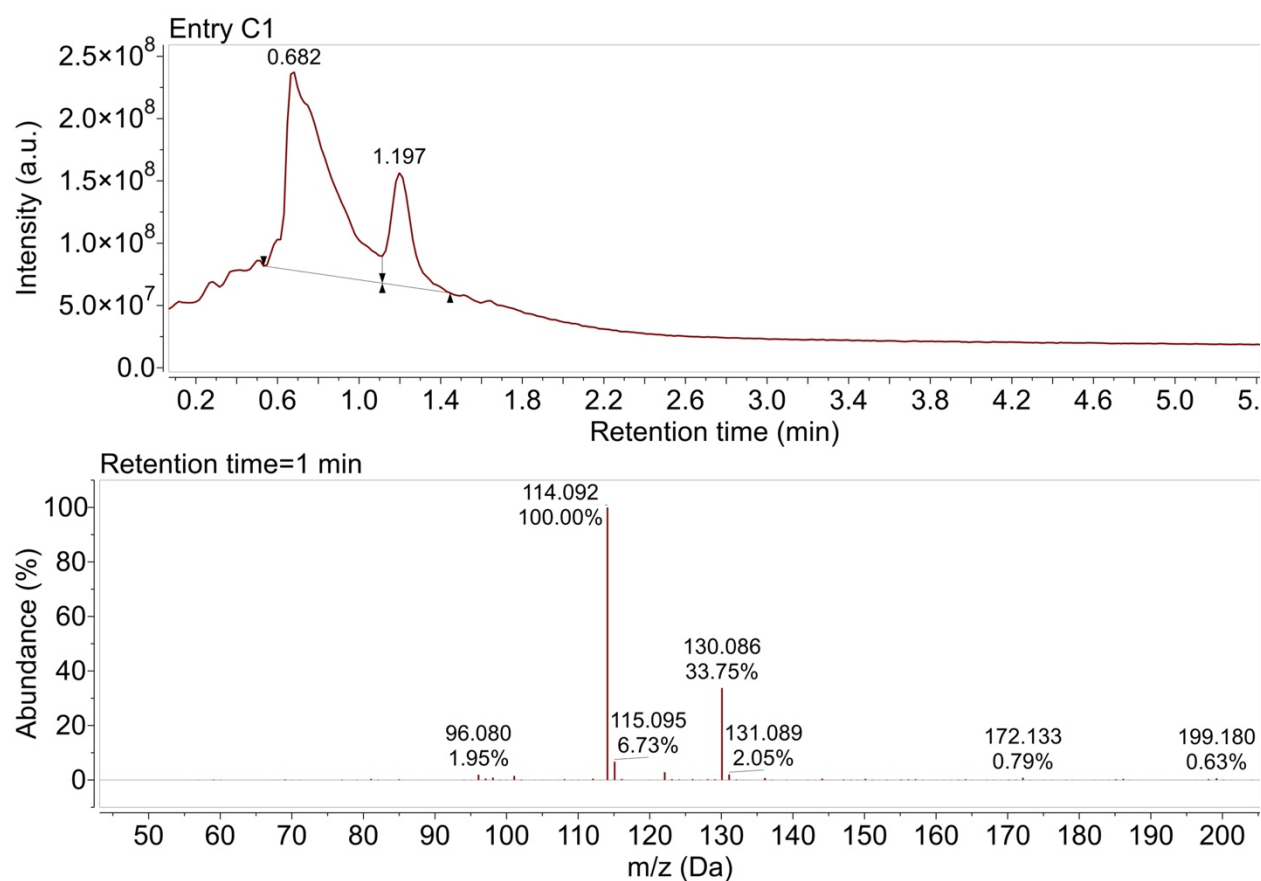
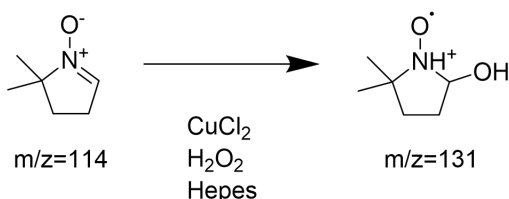


*Figure S12: Mass spectrum of Table 4, entry C1 (main text). MS profile for RT = 1 min*

### c. DMPO-Hydroxyl adduct Positive Control

In a 10 mL oven dried round bottom flask were combined  $\text{H}_2\text{O}_2$  (5.0 mL, 10 mM aq) and copper(II) chloride (400  $\mu\text{g}$ , 3.0  $\mu\text{mol}$ ) to make  $[\text{Cu}] = 0.6 \text{ mM}$ . Hepes buffer (Alfa Aesar), solid, 3.0 mg, to make 2.5 mM was added into the solution. The resulting solution was stirred for two minutes at room temperature before DMPO (15 mg, 130  $\mu\text{mol}$ , to make 27 mM) was added. An aliquot was recovered for analysis after 45 minutes.



*Scheme S3: DMPO-hydroxyl adduct positive control experiment*

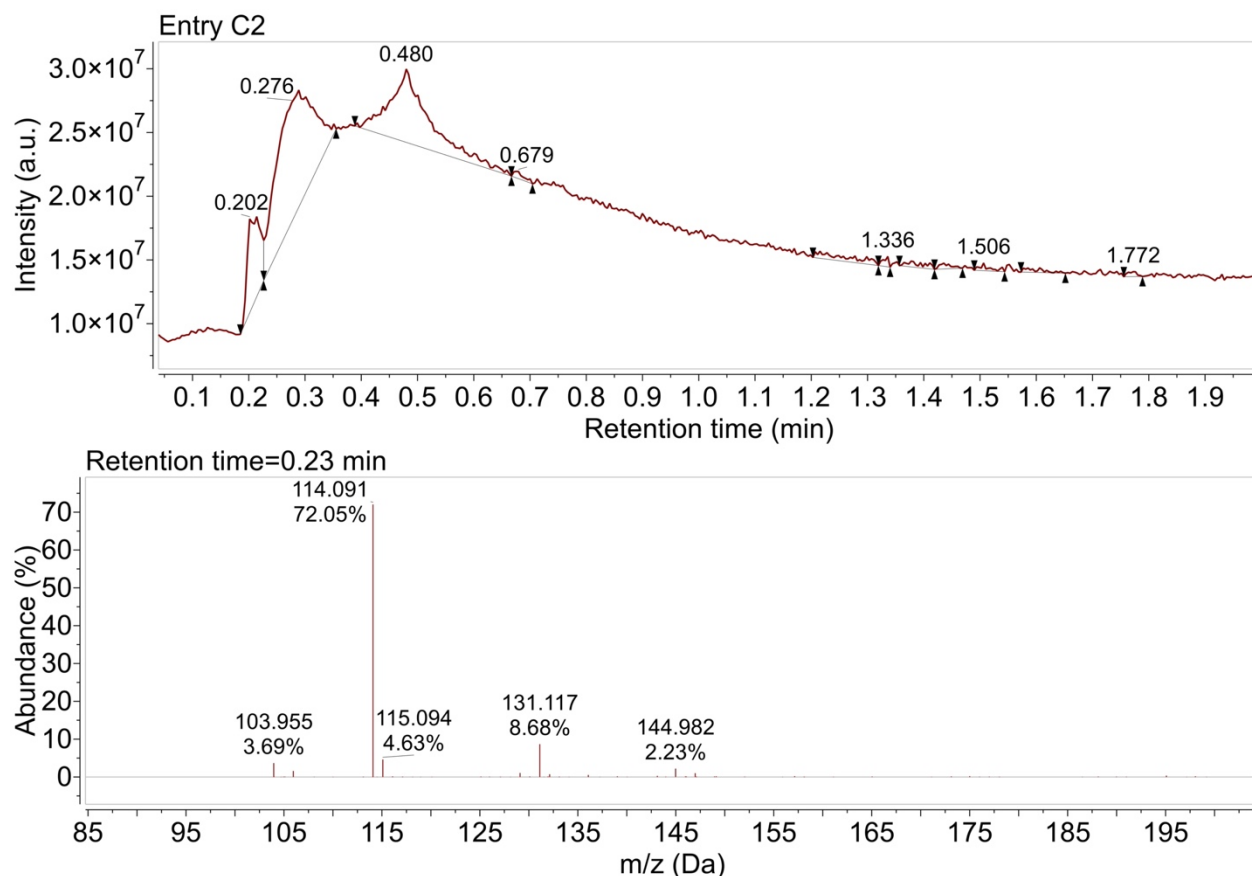
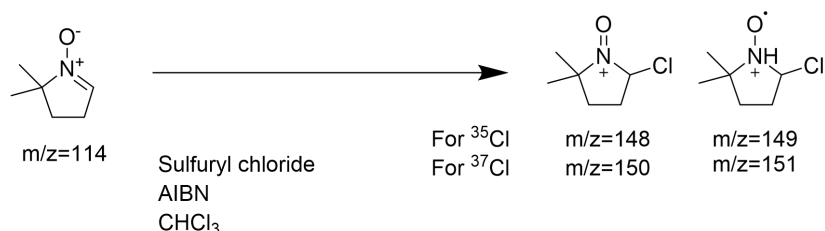


*Figure S13: Mass spectrum of Table 4, entry C2(main text). MS profile for RT=0.23 min*

#### d. DMPO-Chlorine adduct Positive Control

In a 25 mL oven dried round bottom flask were combined chloroform (10 mL), sulfonyl chloride (2.0 mL, 25 mmol, 2.5 M), and azobisisobutyronitrile (AIBN, 10 mg, 61  $\mu$ mol). The vessel was purged with nitrogen gas, a condenser was attached, and the solution was heated to 55 °C. After two minutes DMPO (15 mg, 13  $\mu$ mol, 13 mM) was added. An aliquot was recovered for analysis after 20 minutes.



*Scheme S4: DMPO-chlorine adduct positive control experiment*

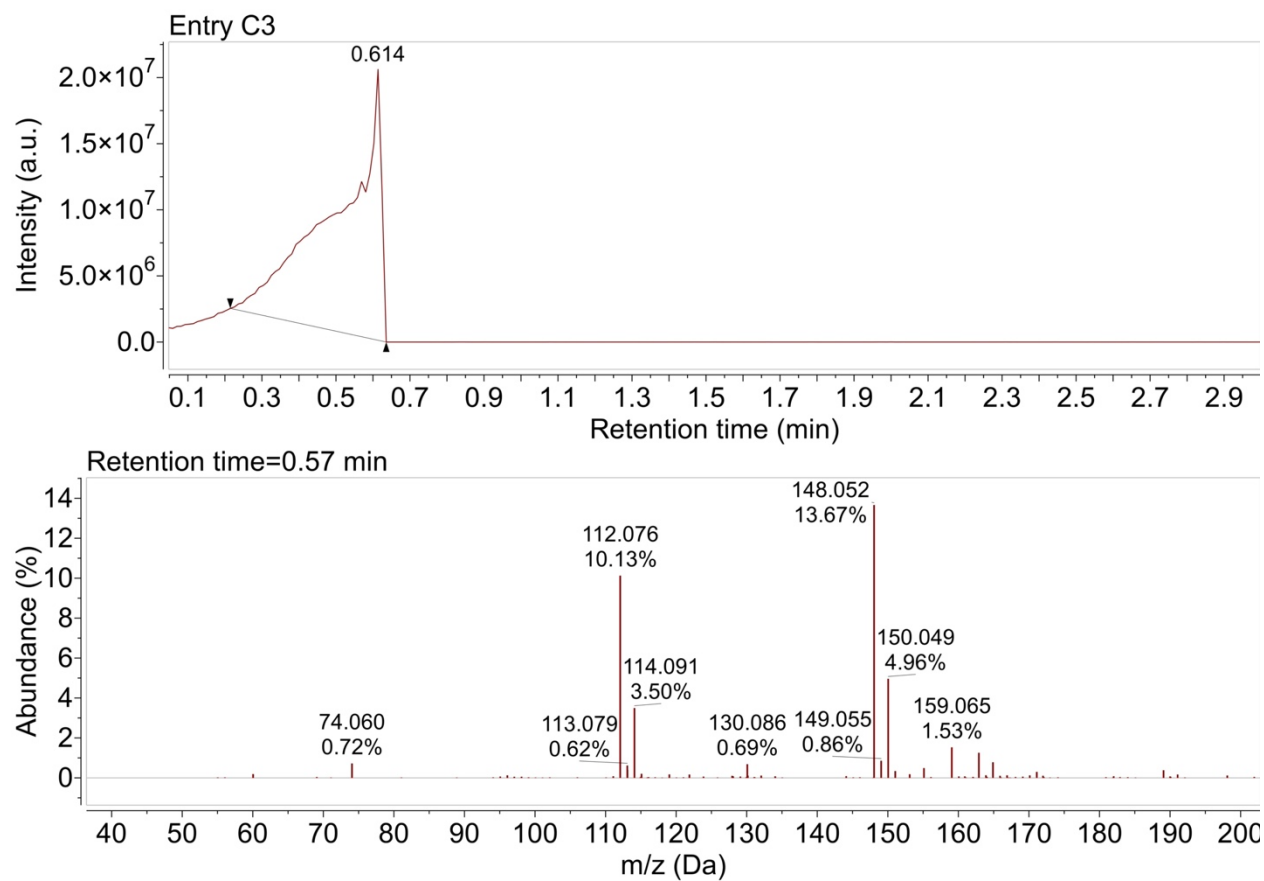


*Figure S14: Mass spectrum of Table 4, entry C3 (main text). MS profile for RT=0.57 min.*

## 8. GC analysis of electrolysis headspace

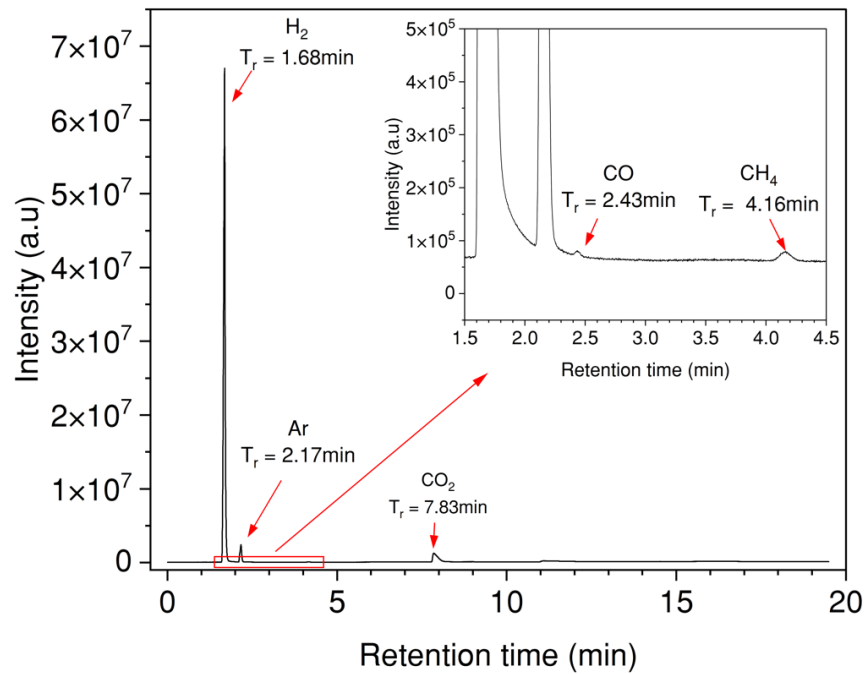


Figure S15: GC of electrolysis set-up headspace

**9. Supporting NMR spectrum for active radical detection experiments:**

**a.  $^1\text{H}$  NMR spectrum of 3,3'-sulfonylbis(*N,N*-dibutylaniline) (Bu<sub>4</sub>DDS)**

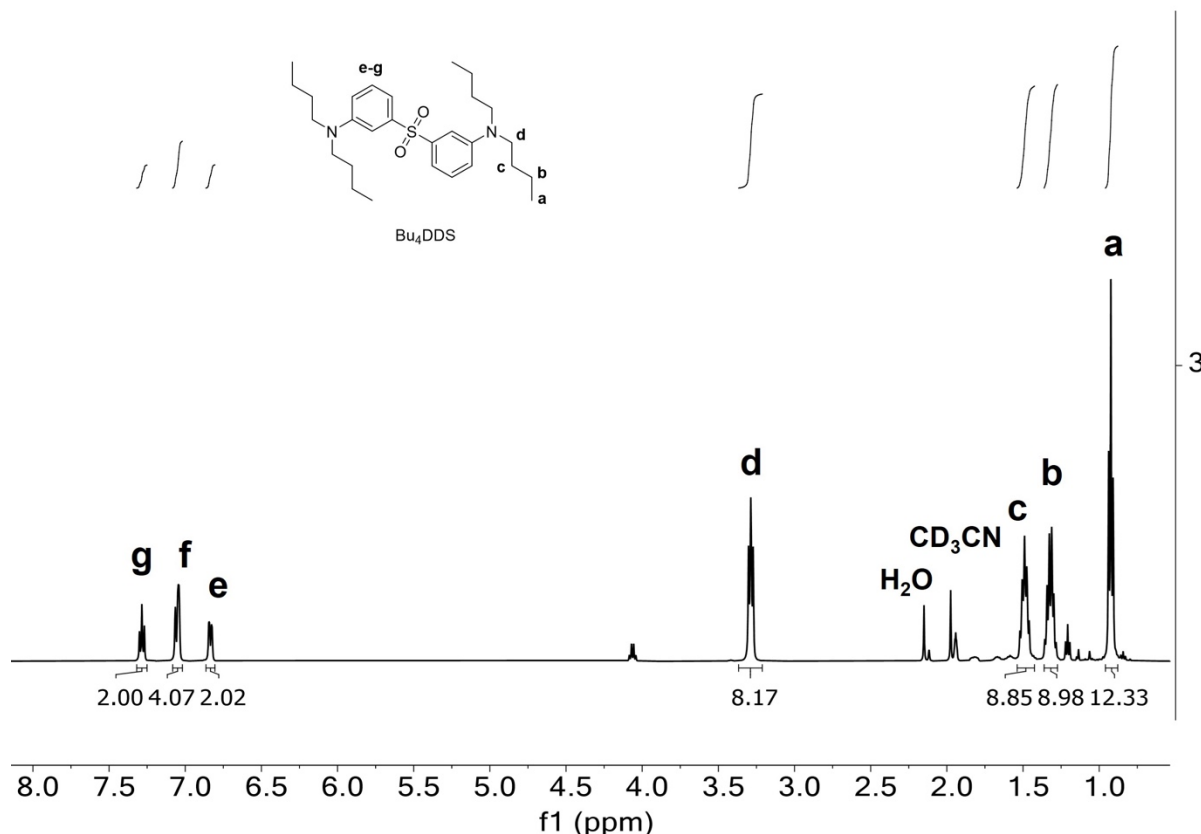


Figure S16:  $^1\text{H}$  NMR spectrum of Bu<sub>4</sub>DDS matrix model

$^1\text{H}$  NMR (500 MHz,  $\text{cd}_3\text{cn}$ )  $\delta$  7.28 (t,  $J = 8.0$  Hz, 2H), 7.08 – 7.02 (m, 4H), 6.83 (dd,  $J = 8.5, 2.7$  Hz, 2H), 3.29 (t,  $J = 7.6$  Hz, 8H), 1.49 (p,  $J = 7.6$  Hz, 9H), 1.32 (h,  $J = 7.4$  Hz, 9H), 0.92 (t,  $J = 7.4$  Hz, 12H).

$^{13}\text{C}$  NMR (100 MHz,  $\text{cd}_3\text{cn}$ )  $\delta$  148.49, 142.76, 130.08, 115.72, 112.74, 109.11, 50.25, 28.77, 19.84, 13.27.

FR-IR (thin film)  $\nu = 1187$  (C-N), 1497 (CH<sub>2</sub>), 1597 (C=C), 1305, 1153 (S=O)  $\text{cm}^{-1}$ .

Q-TOF MS  $m/z = \text{C}_{28}\text{H}_{44}\text{N}_2\text{O}_2\text{S}$ , calculated mass 472, found protonated mass  $[\text{C}_{28}\text{H}_{45}\text{N}_2\text{O}_2\text{S}]^{1+}$  473.321 g/mol.

### b. $^1\text{H}$ NMR stacked spectra of $\text{Bu}_4\text{DDS}$ digestion in electrolyzed system

In our glass electrolysis vessel (main text scheme 2 and figure S1) were combined acetic acid (10.0 mL, 17.4 M) in water (5.0 mL) and NaCl (877 mg, 1M). A voltage of 4V was applied, then  $\text{Bu}_4\text{DDS}$  was added (30 mg, 4.2 mmol, to make 64  $\mu\text{M}$ ). The solution was heated to 65°C for 60 minutes before the first sample was collected. After 120 minutes, a second sample was collected. The voltage was disconnected 5 minutes thereafter.

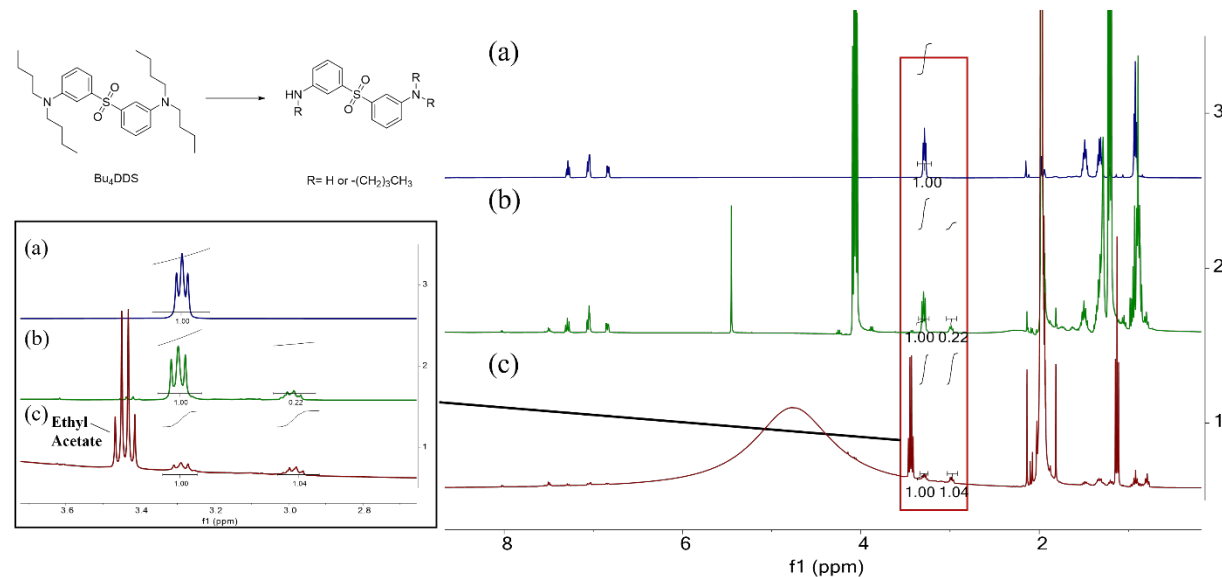


Figure S17: Stacked  $^1\text{H}$  NMR spectra of (a)  $\text{Bu}_4\text{DDS}$ , (b) Table 5 entry B1, and (c) entry B2 from the main text

### c. $^1\text{H}$ NMR stacked spectra of DDS digestion in electrolyzed system

In our glass electrolysis vessel (main text scheme 2 and figure S1) were combined acetic acid (10.0 mL, 17.4 M) in water (5.0 mL) and NaCl (877 mg, 1M). A voltage of 4V was applied, then DDS (5.0 g, 20 mmol, to make 1.3M) was added into the solution. The solution was heated to 65°C. After 60 minutes, the first sample aliquot was collected. A second was collected after 300 minutes. The voltage was disconnected 5 minutes thereafter.

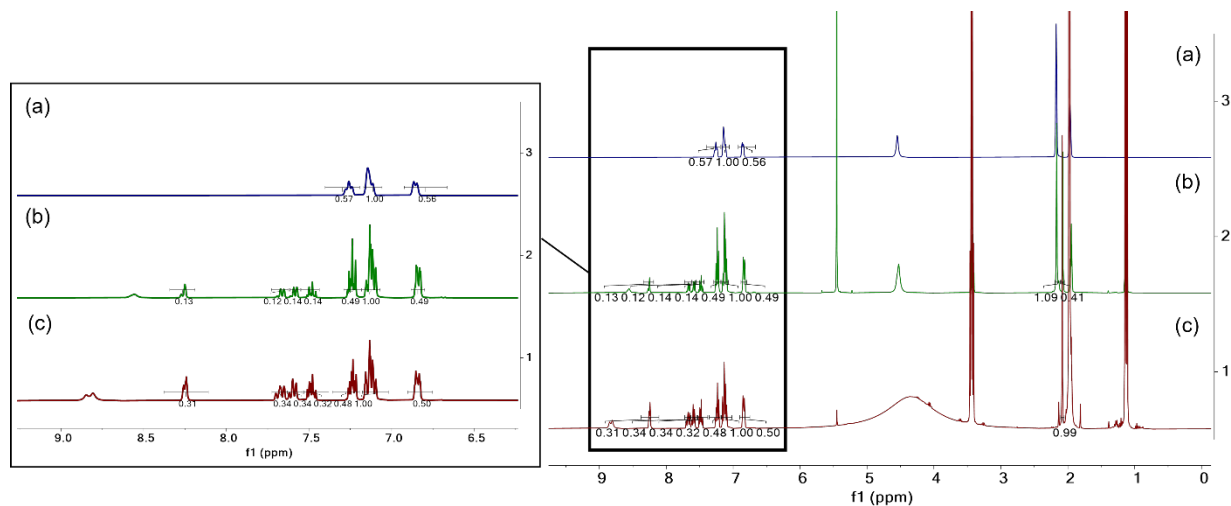
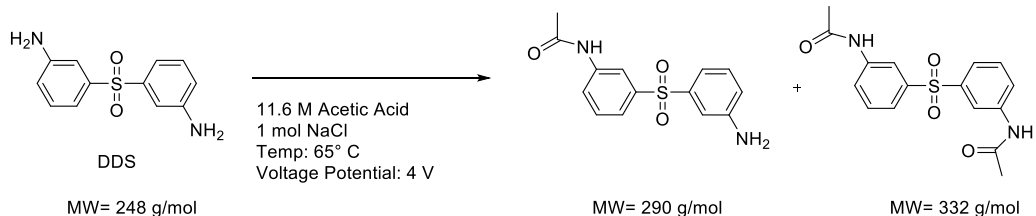


Figure S18: Stacked <sup>1</sup>H NMR spectra of (a) 3,3'-diaminodiphenylsulfone (DDS), DDS in electrolysis digestion conditions for (b) 1 hour (b), and (c) 5 hours

**d. MS spectrum of DDS digestion in electrolyzed system for 1 hour**



Scheme S5: Proposed DDS acylation reaction

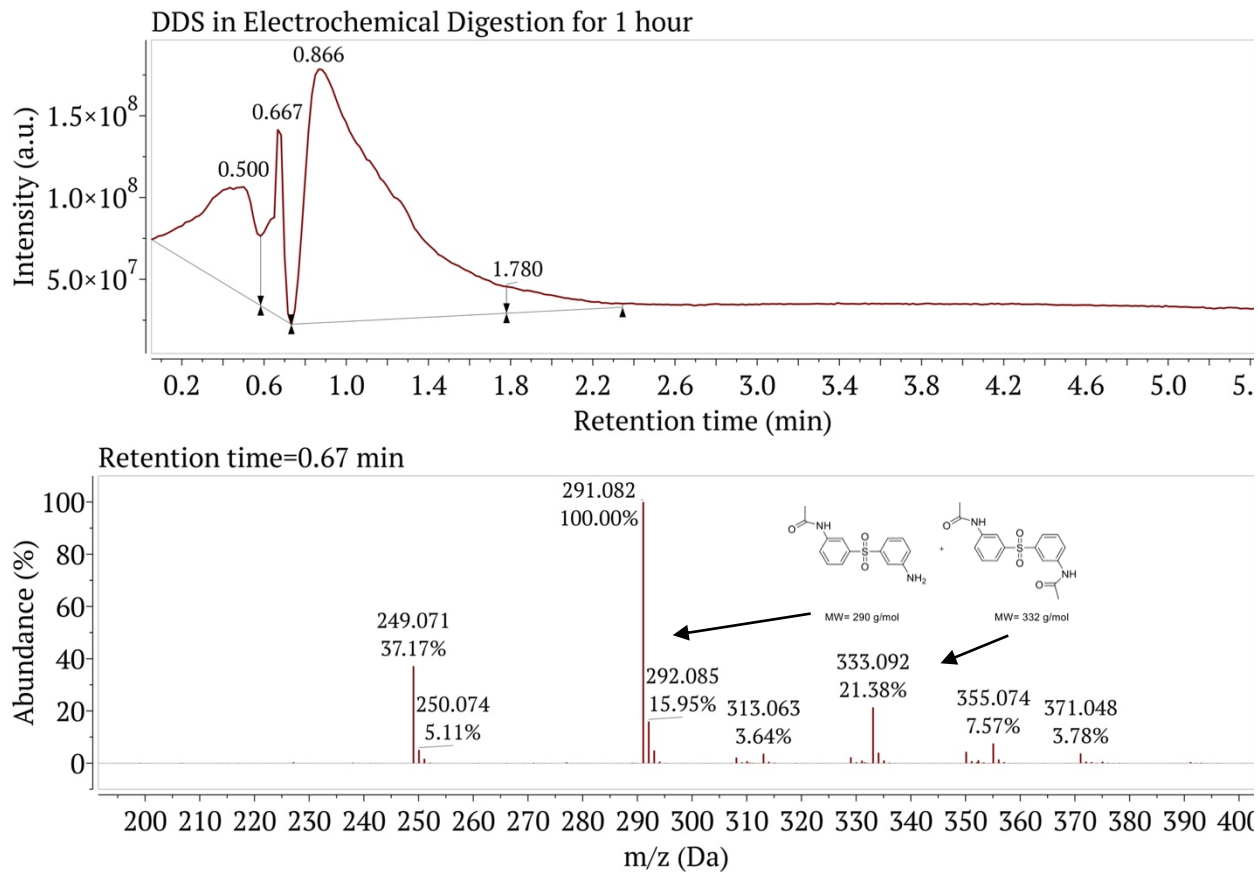


Figure S19: LC-QTOF mass profile of DDS in electrolysis digestion conditions for 1 hour.

The molecule DDS undergoes an acylation reaction with the solvent to form both the mono and bis amide.